

The global gas and dust budget of the Small Magellanic Cloud

M. Matsuura, Paul M. Woods, P.J. Owen

Department of Physics and Astronomy, University College London, Gower Street, London WC1E 6BT, United Kingdom

Submitted

ABSTRACT

In order to understand the evolution of the interstellar medium (ISM) of a galaxy, we have analysed the gas and dust budget of the Small Magellanic Cloud (SMC). Using the *Spitzer Space Telescope*, we measured the integrated gas mass-loss rate across asymptotic giant branch (AGB) stars and red supergiants (RSGs) in the SMC, and obtained a rate of $1.4 \times 10^{-3} M_{\odot} \text{ yr}^{-1}$. This is much smaller than the estimated gas ejection rate from type II supernovae (SNe) ($2\text{--}4 \times 10^{-2} M_{\odot} \text{ yr}^{-1}$). The SMC underwent an increase in starformation rate in the last 12 Myrs, and consequently the galaxy has a relatively high SN rate at present. Thus, SNe are more important gas sources than AGB stars in the SMC. The total gas input from stellar sources into the ISM is $2\text{--}4 \times 10^{-2} M_{\odot} \text{ yr}^{-1}$. This is slightly smaller than the ISM gas consumed by starformation ($\sim 8 \times 10^{-2} M_{\odot} \text{ yr}^{-1}$). Starformation in the SMC relies on a gas reservoir in the ISM, but eventually the starformation rate will decline in this galaxy, unless gas infalls into the ISM from an external source. The dust injection rate from AGB and RSG candidates is $1 \times 10^{-5} M_{\odot} \text{ yr}^{-1}$. Dust injection from SNe is in the range of $0.2\text{--}11 \times 10^{-4} M_{\odot} \text{ yr}^{-1}$, although the SN contribution is rather uncertain. Stellar sources could be important for ISM dust ($3 \times 10^5 M_{\odot}$) in the SMC, if the dust lifetime is about 1.4 Gyrs. We found that the presence of poly-aromatic hydrocarbons (PAHs) in the ISM cannot be explained entirely by carbon-rich AGB stars. Carbon-rich AGB stars could inject only $7 \times 10^{-9} M_{\odot} \text{ yr}^{-1}$ of PAHs at most, which could contribute up to $100 M_{\odot}$ of PAHs in the lifetime of a PAH. The estimated PAH mass of $1800 M_{\odot}$ in the SMC can not be explained. Additional PAH sources, or ISM reprocessing should be needed.

Key words: galaxies: evolution – galaxies: individual: the Magellanic Clouds – (ISM:) dust, extinction – stars: AGB and post-AGB – stars:mass-loss – (stars:) supernovae: general

1 INTRODUCTION

Stars and the interstellar medium (ISM) of galaxies experience a constant exchange of gas and dust. Stars are formed in molecular clouds in the ISM, and evolve. Elements are synthesised in stellar interior, and eventually they are ejected at the end of the stellar life. Gas ejected by stars is enriched with metals, in comparison to with the gas where the stars were initially formed. Dust grains are formed around evolved stars and supernovae (SNe) and they are injected into the ISM. They might be processed in the ISM, though that remains uncertain. Eventually, dust grains are destroyed by shocks generated by SN blast winds. The lifecycle of matter drives the evolution of the ISM, and ultimately, the evolution of galaxies.

The concept of the lifecycle of matter, in particular gas content, is well accepted and has been adopted in the chemical evolution models and stellar population models of galaxies (e.g. Pagel & Tautvaisiene 1998; Bruzual & Charlot 2003; Kodama & Arimoto 1997). However, it had been difficult to actually measure the gas and dust feedback from stars into the ISM in real terms. The *Spitzer*

Space Telescope (Werner et al. 2004) has provided an opportunity to measure the gas feedback from stars in the Magellanic Clouds (Matsuura et al. 2009; Srinivasan et al. 2009; Boyer et al. 2012), delivering new constraints on chemical evolution models.

Dust is one of the important contents of galaxies. Dust absorbs energy emitted from stars within a galaxy, and re-emits it in the infrared to sub-mm wavelengths. The presence of dust controls the energy input and output from the ISM of galaxies, and affects the spectral shape of the galaxy and the underlining physics of the ISM (Galliano et al. 2005; Dunne et al. 2011).

Despite such an important role in the physics of the ISM and galaxies, it is still not well established how dust mass in the ISM evolves (Sloan et al. 2009; Draine 2009; Tielens et al. 2005; Calura et al. 2008). This requires detailed studies of the dust formation and destruction processes in stars and the ISM. Dust grains are considered to be formed in a wide range of objects, particularly stars in the late phase of evolution (e.g. Gehr 1989). Such theoretical studies have been conducted (Nozawa et al.

2003; Morgan & Edmunds 2003; Ferrarotti & Gail 2006; Zhukovska et al. 2008; Valiante et al. 2009) but are poorly constrained by observations at present. Once grains are ejected from stars into the ISM, it has been proposed that dust grains are re-processed and destroyed. Dust grains might grow in the ISM, using stellar dust as seeds (e.g. Tielens et al. 2005; Draine 2009), but it is more difficult to directly measure these processes. This paper focuses on establishing an understanding of what the contribution of stellar dust is to the evolution of dust in the ISM.

One of the important dust sources are asymptotic giant branch (AGB) stars, low- and intermediate-mass ($1-8 M_{\odot}$) evolved stars. It has been well established that dust grains are formed in the AGB outflow (e.g. Habing 1996). However, it is challenging to make a quantitative analysis; namely to measure dust formed in evolved stars in entire populations across galaxies, and evaluate their contribution to dust in the ISM, because this requires a large survey of AGB stars in a galaxy. One of the pioneering studies was based on the IRAS survey of the solar neighbourhood (Jura & Kleinmann 1989), and the Spitzer Space Telescope opened up a possibility for such studies beyond the Milky Way (Matsuura et al. 2009; Srinivasan et al. 2009).

High-mass stars are considered to form dust in various evolutionary stages, such as red supergiants (RSGs), Wolf-Rayet stars, luminous blue variables (LBVs), and supernova (SNe). Due to limited number of sample, the mass dust formed in high mass stars, and in particular, SNe, is uncertain. Recent *Spitzer* and *Herschel* studies of SNe and SN remnants (SNRs) show that type-II SNe can form dust, but the reported dust masses range from 10^{-4} to $\sim 1 M_{\odot}$ (Sugerman et al. 2006; Meikle et al. 2007; Barlow et al. 2010; Matsuura et al. 2011; Gomez et al. 2012). Type-Ia SNe, which have an origin in low- and intermediate-mass binary stars, appear to form very small amounts of dust (Gomez et al. 2012).

The explosion of high mass stars creates expanding winds, which often have multiple velocity components (Kjær et al. 2010). When the fast blast wind collides with the ISM dust, ISM dust grains can be destroyed via sputtering and shattering processes (Jones et al. 1996). The lifetime of dust is determined by its destruction by SN shocks. Assuming homogeneous gas and dust distributions, the lifetime of dust is estimated to be nearly 1 Gyr (Jones et al. 1996). Gas and dust are distributed inhomogeneously in the ISM, so as it is very difficult to estimate a precise dust lifetime.

In this paper, we measure the gas and dust injection rate from AGB stars and RSGs in the Small Magellanic Cloud (SMC). This galaxy is only 56 kpc away (McCumber et al. 2005) and is a molecular-poor galaxy, yet has some ongoing starformation. The measured gas and dust masses ejected from AGB stars and RSGs are compared with masses ejected from SNe, and with the starformation rate in the SMC. We discuss the current problems in understanding the gas and dust budget, and its evolution in these galaxies.

2 MASS-LOSS RATES OF AGB STARS AND RED SUPERGIANTS

Mass-loss rates of AGB stars and red supergiants correlate well with infrared excess. Often near-infrared photometric

points are used to represent the photospheric flux, while mid-infrared fluxes illustrate the emission from the dust thermal emission. Taking near- and mid-infrared colours is an indicator of mass-loss rates (Le Bertre & Winters 1998; Whitelock et al. 1994).

The correlation between colour and mass-loss rates have been established for LMC and SMC carbon-rich AGB stars (Matsuura et al. (2009), who used the mass-loss measurements from Groenewegen et al. (2007), and photometric data from Meixner et al. (2006) and Skrutskie et al. (2006)). The resultant relations were

$$\log \dot{M}_g = -6.20/([3.6] - [8.0]) + 0.83 - 3.39 \quad (1)$$

in the range of $1 < [3.6] - [8.0] < 9$

$$\log \dot{M}_g = -14.50/(K_s - [8.0]) + 3.86 - 3.62 \quad (2)$$

in the range of $1 < K_s - [8.0] < 9$, where \dot{M}_g is the gas mass-loss rate.

The relation for $K_s - [24]$ for the same data set is found to be

$$\log \dot{M}_g = -20.25/(K_s - [24]) + 4.98 - 3.47, \quad (3)$$

We further derive the relationship for oxygen-rich stars, using Groenewegen et al. (2009)'s analysis of oxygen-rich AGB stars and red supergiants in the Magellanic Clouds. We correlate their photometric data with Spitzer and 2MASS data (Gordon et al. 2011). The resultant correlation is found in Fig. 1, and the fits to these data are given as

$$\log \dot{M}_g = -18.97/([3.6] - [8.0]) + 2.698 - 0.9954 \quad (4)$$

in the range of $1 < [3.6] - [8.0] < 3$

$$\log \dot{M}_g = -12.28/(K_s - [8.0]) + 2.297 - 2.888 \quad (5)$$

in the range of $1 < K_s - [8.0] < 7$, and

$$\log \dot{M}_g = -38.96/(K_s - [24]) + 4.903 - 1.522, \quad (6)$$

in the range of $1 < K_s - [24] < 9$.

It is difficult to measure the mass-loss rates of stars with very little infrared excess and blue colour cut-offs. However, contributions from very low-mass loss rate stars are not important for the overall global gas and dust budget (Le Bertre et al. 2001; Matsuura et al. 2009).

3 OBJECT CLASSIFICATIONS

The first step is to understand the infrared photometric survey and classify the point sources. Colour magnitude diagrams (CMDs) and colour-colour diagrams (CCDs) are commonly used to classify the point sources (e.g. Blum et al. 2006; Ita et al. 2008; Woods et al. 2011). In this work, we use the LMC objects to set object classifications based on a CMD and a CCD, and apply the classification method to SMC objects.

In our previous study, we focused on classification based on $[3.6]-[8.0]$ v.s. $[8.0]$ CMD to extract carbon-rich AGB stars (Matsuura et al. 2009). We are going to revise this classification, and particularly optimise the classifications for high mass-loss rate AGB stars, which are dominant for the gas and the dust budget.

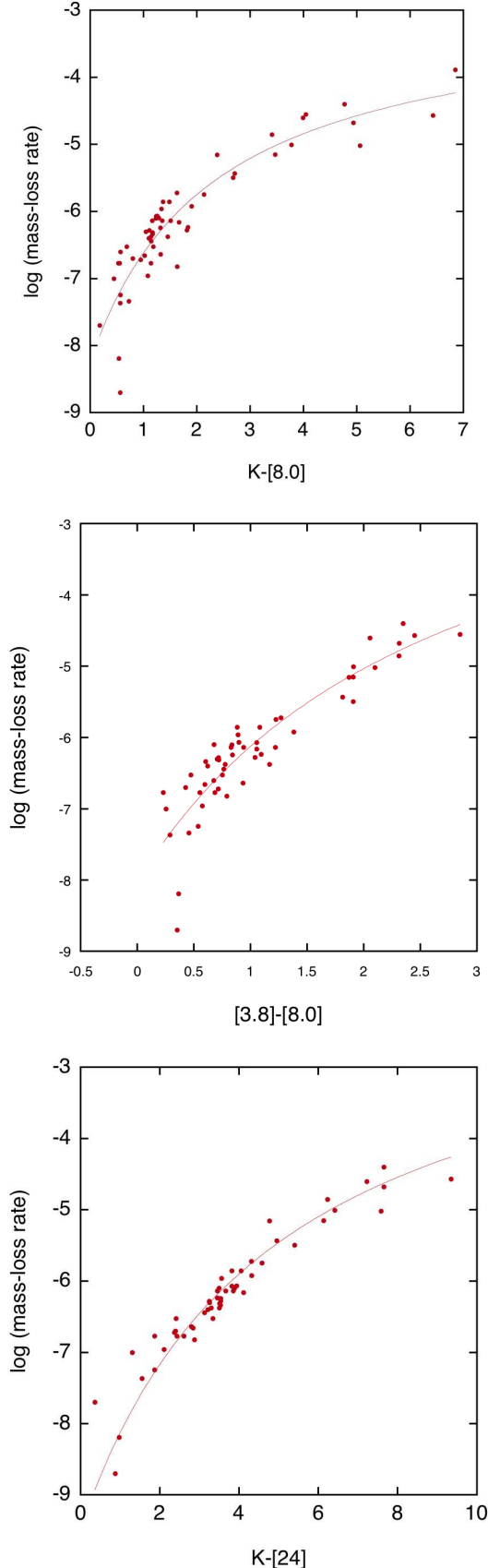


Figure 1. Correlation between mass-loss rate (in $M_{\odot} \text{ yr}^{-1}$) and colour for oxygen-rich AGB stars and RSGs

3.1 Cross-identifications

We start the object classification process by cross-identifying the LMC photometric data with spectroscopically known objects in the LMC.

Matsuura et al. (2009) have assembled the LMC objects with spectroscopical classifications and we use these sample: Sample of M-type giants and supergiants, carbon-rich stars, planetary nebulae are assembled from Kontizas et al. (2001), Cioni et al. (2001), Sanduleak & Philip (1977), Blanco et al. (1980), Westerlund et al. (1981), Wood et al. (1983), Wood et al. (1985), Hughes (1989) and Reid et al. (1988). We added samples of Wolf Rayet (WR) stars (Breysacher et al. 1999) and S Dor variables (Luminous Blue Variables (LBVs); Van Genderen 2001), post-AGB stars (Gielen et al. 2009; Volk et al. 2011; Matsuura et al. 2011), and planetary nebulae (Woods et al. 2011; Matsuura et al. 2011).

3.2 Object classifications

3.2.1 LMC colour-magnitude diagram

Figure 2 shows the $[3.8]-[8.0]$ vs $[8.0]$ CMDs of the LMC objects. This diagram was used for object classifications of carbon-rich AGB stars and oxygen-rich AGB stars/red supergiants in our previous study (Matsuura et al. 2009). The black lines shows the separation of these two types. LMC Spitzer spectroscopic observations (Kemper et al. 2010) confirm that this classification is effective (Woods et al. 2011).

This CMD classification is simple and largely correct. Actually, contamination of a small number of red objects (carbon-rich post-AGB stars and PNe and distant galaxies) into AGB stars and RSGs could potentially change the analysis of the global gas and dust budget, which is the final aim of this paper. The further and more severe problem is contamination of a few, but high mass-loss rate oxygen-rich AGB stars which fall into the carbon-rich AGB region at about $[3.6]-[8.0] \sim 2$ and $[8.0] \sim 6$ mag. We introduce one more step in the analysis, as described in Sect. 3.2.2, to minimise these contaminations.

Many point sources are found in the region between $2 < [3.6] - [8.0] < 4$ and $[8.0] < 12$. This is associated with distant galaxies (Kozłowski & Kochanek 2009).

3.2.2 LMC colour-colour diagram

In order to improve object classifications further, we introduce another colour-colour diagram, the $K-[8.0]$ vs $K-[24]$ of the LMC objects, as plotted in Fig. 3.

Prior to the plot, point sources associated with distant galaxies (Kozłowski & Kochanek 2009) were removed. We defined their distribution as $[3.6] - [8.0] > 2.0$ and $[8.0] < 10$ from Fig. 2. These galaxies would appear approximately between $1.5 < K - [8.0] < 2.5$ and $5 < K - [24] < 7$ in the CCD, if they had been plotted.

We overlay the mass-loss vs colour relationship derived in Sect. 2 on top of the CMD. There are two separate sequences for oxygen-rich and carbon-rich objects. The redder the colour, the higher the mass-loss rate, in general, as the equations show.

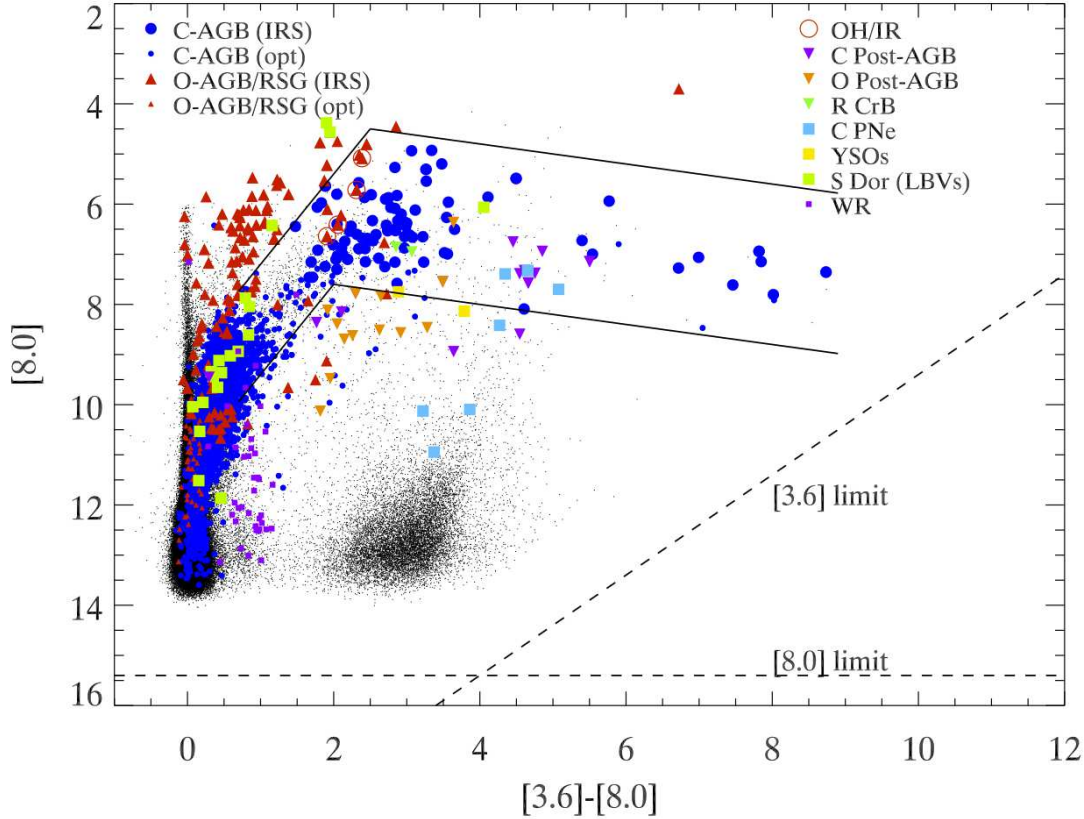


Figure 2. The infrared colour-magnitude diagram of the LMC objects. Dots represent all point sources obtained from the SAGE catalogue (Meixner et al. 2006). Circles show the spectroscopically identified carbon-rich AGB stars. Upward-pointing triangles show oxygen-rich AGB stars and red supergiants (RSGs). In addition to the AGB stars, S Dor type variables (luminous blue variables), and Wolf Rayet (WR) stars are plotted. The dashed lines show the expected detection limit of the final SAGE catalogue.

We use this CCD and the CMD to classify objects. We cross check the reliability of these classifications with SIMBAD. We found that the contaminations are not a big issue for the LMC gas and dust budget, but it does change slightly (10%) for the SMC. A cross-check with SIMBAD found that non-AGB red objects that contaminated the AGB stars are, if they have known identifications, PNe (Henize 1955) and YSO candidates (Bolatto et al. 2007).

3.2.3 SMC colour-magnitude diagram

Once we establish the object classifications using the LMC objects, we apply the same method to the SMC objects.

Figure 4 shows the CMD of SMC point-sources extracted from the SAGE-SMC catalogue (Gordon et al. 2011). The black lines show the separation between carbon-rich AGB stars and oxygen-rich AGB stars/red supergiants, which was derived from LMC objects, but are scaled by the difference of distance moduli between these two galaxies. The distance moduli of the LMC and the SMC are 18.5 and 18.9 mag respectively (Nikolaev & Weinberg 2000; Westerlund 1990), so that the separation line was shifted by 0.4 magnitude fainter in [8.0] for the SMC objects.

There is a clear difference in LMC and SMC CMDs: fewer red stars are found in the SMC than the LMC. Similarly, there are only three carbon-rich candidates with very red colours ($[3.6]-[8.0] > 5.0$), whereas there are 33 such

stars in the LMC. We take into account the difference in the number of stars in these two galaxies. Taking the absolute V -band magnitude as a measure of number of stars in a galaxy, the SMC should have about 7 times fewer stars than the LMC (Westerlund 1990). The difference in the red carbon-rich AGB stars appears to be slightly larger than the difference in the number in the stars, but this is not conclusive.

3.2.4 SMC colour-colour diagram

Figure 5 shows the same combination of CCD as Fig. 3, but for the Small Magellanic Cloud (SMC). There is a slight difference in the distributions of stars compared with the LMC diagram: the SMC has very few oxygen-rich AGB stars with colour redder than $K - [8.0] > 1.8$. This corresponds to approximately a mass-loss rate higher than $10^{-6} M_{\odot} \text{ yr}^{-1}$.

The SMC CCD shows that there are a reasonable number of stars found in region (a), which are carbon-rich AGB candidates. Oxygen-rich AGB stars, represented by region (b), are relatively scarce. There are even fewer oxygen-rich AGB stars in the SMC than the LMC (Fig. 3).

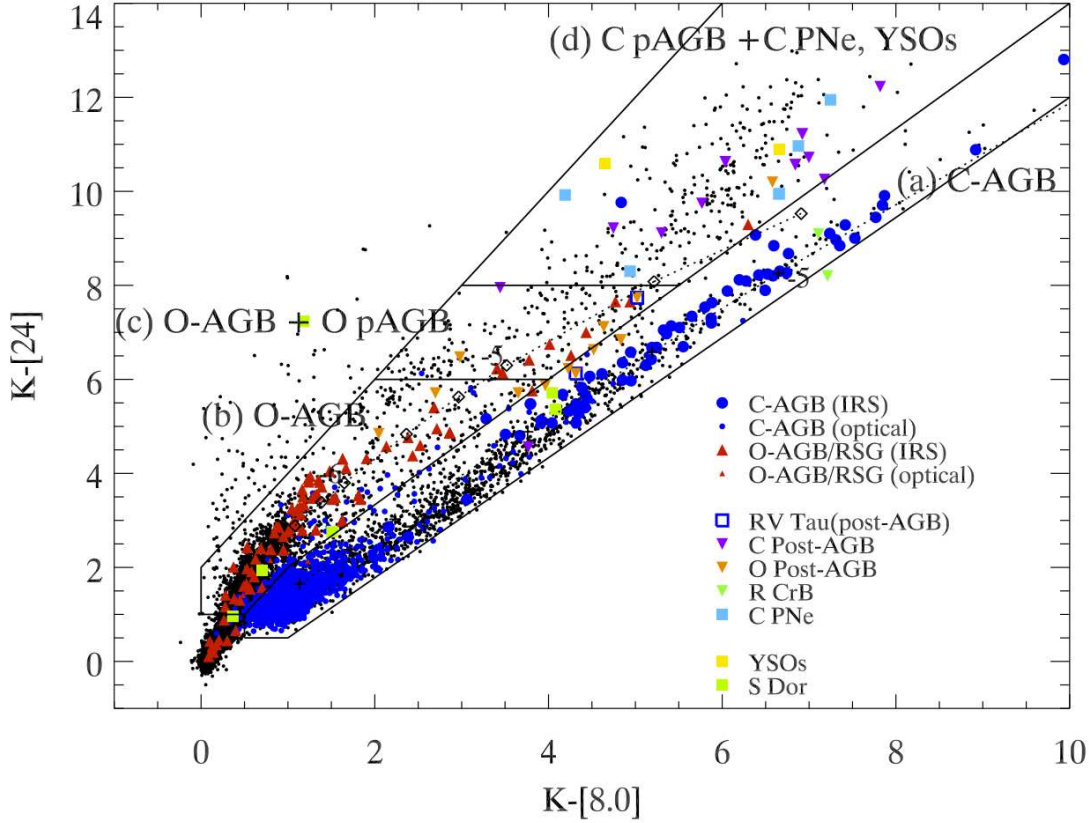


Figure 3. Colour-colour diagram of the point sources in the LMC. The objects with spectroscopic classifications are marked with symbols. We divide the colour-colour diagram into 4 regions (a)–(d) and dominant types of objects in these regions are indicated. Oxygen-rich stars and carbon-rich stars follow two separate sequences. Two dashed lines show the estimated mass-loss rate and colour relations for oxygen-rich and carbon-rich stars, respectively, and they are calculated from equations (1)–(6). The numbers alongside the lines show the mass-loss rates in log-scale (Sect.2).

Table 1. Gas and dust injected into the ISM of the LMC and the SMC

Sources	LMC		SMC	
	Gas ($10^{-2} M_{\odot} \text{ yr}^{-1}$)	Dust ($10^{-5} M_{\odot} \text{ yr}^{-1}$)	Gas ($10^{-2} M_{\odot} \text{ yr}^{-1}$)	Dust ($10^{-5} M_{\odot} \text{ yr}^{-1}$)
Carbon-rich AGB stars	0.7	4	0.08	0.4
Oxygen-rich AGB + RSGs	0.8	4	0.06	0.3
Type II SNe	6–13	7–400	2–4	2–110
WR stars	~ 0.1		~ 0.01	
OB stars	0.1–1?		~0.03–0.3	
Star-formation rate	20–30		8	

4 GAS AND DUST INJECTION RATE FROM EVOLVED STARS

4.1 Integrated mass-loss rate from AGB stars and red supergiants

Combining the information from object classifications and mass-loss rates from the previous sections, we can estimate the integrated gas and dust mass-loss rates from AGB stars and red supergiants. This is the total gas and dust mass injected from evolved stars into the ISM.

In order to estimate mass-loss rates of individual AGB stars and RSGs, we use the correlation of $[3.6] - [8.0]$ with mass-loss rate. An alternative choice is $K_s - [8.0]$, but some

high mass-loss rate stars are not detected at 2MASS K_s -band, and these stars could contribute a significant fraction to the integrated mass-loss rate from evolved stars.

Object classification is based on $[8.0]$ vs. $[3.6] - [8.0]$ colour, and we supplementary use $K_s - [8.0]$ vs $K_s - [24]$ to remove the contamination of distant galaxies in the red carbon-rich AGB region, as well as high mass-loss rate oxygen-rich AGB stars and RSGs in the carbon-rich AGB region.

By integrating the mass-loss rates of individual AGB stars, we can estimate the total gas and dust inputs from AGB stars and red supergiants into the ISM of the SMC, as summarised in Table 1. The contribution from oxygen-

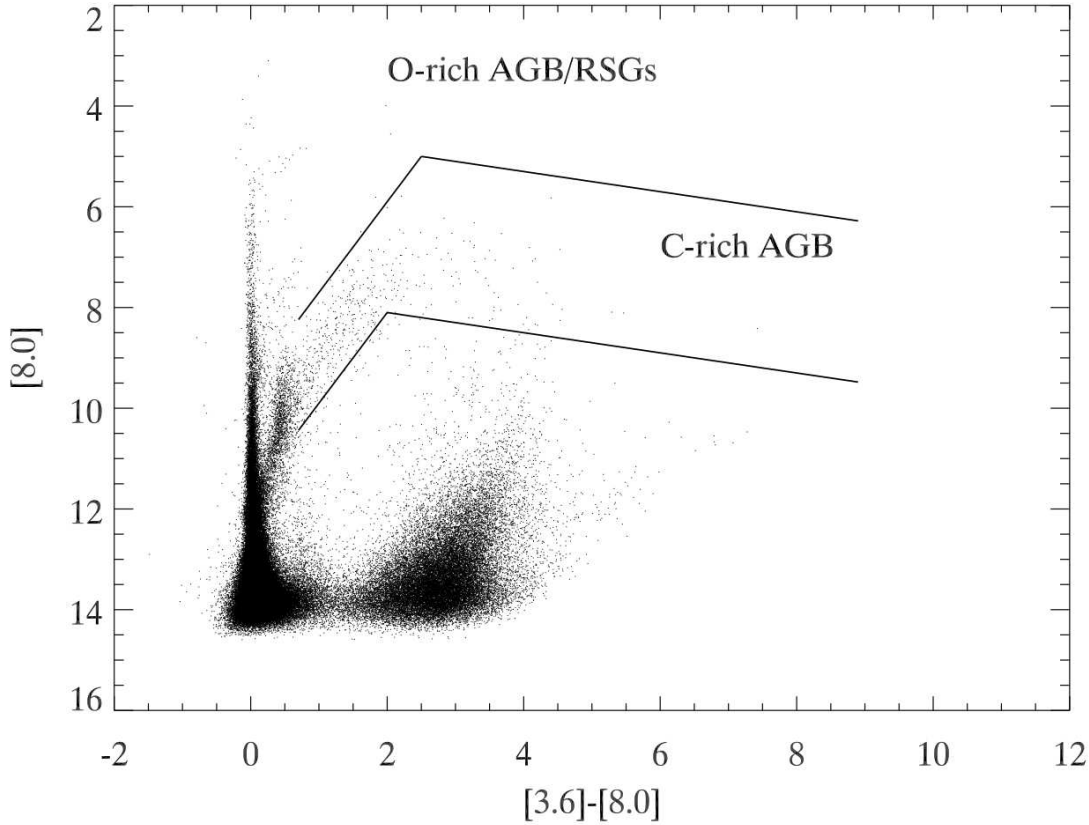


Figure 4. The colour-magnitude diagram of the SMC objects. The regions which are expected to be dominated by carbon-rich AGB stars and oxygen-rich AGB stars and red supergiants are indicated.

rich AGB stars and RSGs contribution is $0.06 \times 10^{-2} M_{\odot} \text{yr}^{-1}$, while carbon-rich AGB stars contribute $0.08 \times 10^{-2} M_{\odot} \text{yr}^{-1}$ in gas. The total gas injection rate from AGB stars and red supergiants is $0.1 \times 10^{-2} M_{\odot} \text{yr}^{-1}$ for the SMC.

The estimated total gas input from evolved stars is $2 \times 10^{-2} M_{\odot} \text{yr}^{-1}$ for LMC. This includes both oxygen-rich and carbon-rich AGB stars and RSGs. In our previous work on the LMC (Matsuura et al. 2009), the integrated mass-loss rate from oxygen-rich AGB stars and RSGs was a crude estimate based on previously known surveys before the SAGE. The current estimation has a slightly higher value. The integrated mass-loss rate is added up, using the contribution from carbon-rich AGB stars ($0.7 \times 10^{-2} M_{\odot} \text{yr}^{-1}$) and oxygen-rich AGB stars and RSGs ($0.8 \times 10^{-2} M_{\odot} \text{yr}^{-1}$).

In the SMC, dust inputs, which are directly measured from mid-infrared observations, are $0.4 \times 10^{-5} M_{\odot} \text{yr}^{-1}$ for carbon-rich AGB and $0.3 \times 10^{-5} M_{\odot} \text{yr}^{-1}$ for oxygen-rich AGB and RSGs.

The gas-to-dust mass ratio is assumed to be 200 for all AGB stars and RSGs as in Groenewegen et al. (2007, 2009). This is the largest uncertainty in our estimate of the integrated gas mass-loss rate. The ratio of 200 is a widely assumed value for the Galactic AGB stars and RSGs, but it is not clear that this ratio is applicable to extra-Galactic evolved stars, where the metallicities of galaxies are different. The gas-to-dust ratio in the ISM and evolved stars is left for future investigations, such as ALMA observations.

Boyer et al. (2012) has estimated that the total dust injection rate is $1 \times 10^{-7} M_{\odot} \text{yr}^{-1}$ from carbon-rich AGB stars,

$6 \times 10^{-7} M_{\odot} \text{yr}^{-1}$ from “extreme-” AGB stars, which they expected to be mostly carbon-rich, and $0.7 \times 10^{-8} M_{\odot} \text{yr}^{-1}$ from oxygen-rich AGB stars, and $3 \times 10^{-8} M_{\odot} \text{yr}^{-1}$ from RSGs. We removed the ambiguity of “extreme” from Boyer et al. (2012)’s classification. We found that the contribution from oxygen-rich AGB stars and red supergiants are much larger than their estimate. Wood et al. (1992) found three OH/IR stars in the SMC. They have not estimated the mass-loss rate of these particular three objects, but the typical range of mass-loss rate of OH/IR stars are $3 \times 10^{-5} - 3 \times 10^{-4} M_{\odot} \text{yr}^{-1}$ (Wood et al. 1992). Wood et al. (1992) estimated these mass-loss rates based on infrared observations, and they adopted a gas-to-dust ratio of 200. The sum of the dust mass-loss rates from these three OH/IR stars alone is estimated to be $2 \times 10^{-7} - 2 \times 10^{-6} M_{\odot} \text{yr}^{-1}$. Groenewegen et al. (2009) analysed the mass-loss rates of AGB stars and RSGs in Magellanic Clouds, and 11 MSX named oxygen-rich SMC stars have a total dust mass loss rate of $4 \times 10^{-7} M_{\odot} \text{yr}^{-1}$. These values show that our estimates are reasonable. This does not affect Boyer et al. (2012)’s overall conclusion that AGB stars and RSGs are not the dominant source of dust in the ISM, which we also found.

4.2 SN gas and dust injection rate

In order to estimate the average gas and dust injection rate from core-collapse SNe into the ISM, we need to estimate

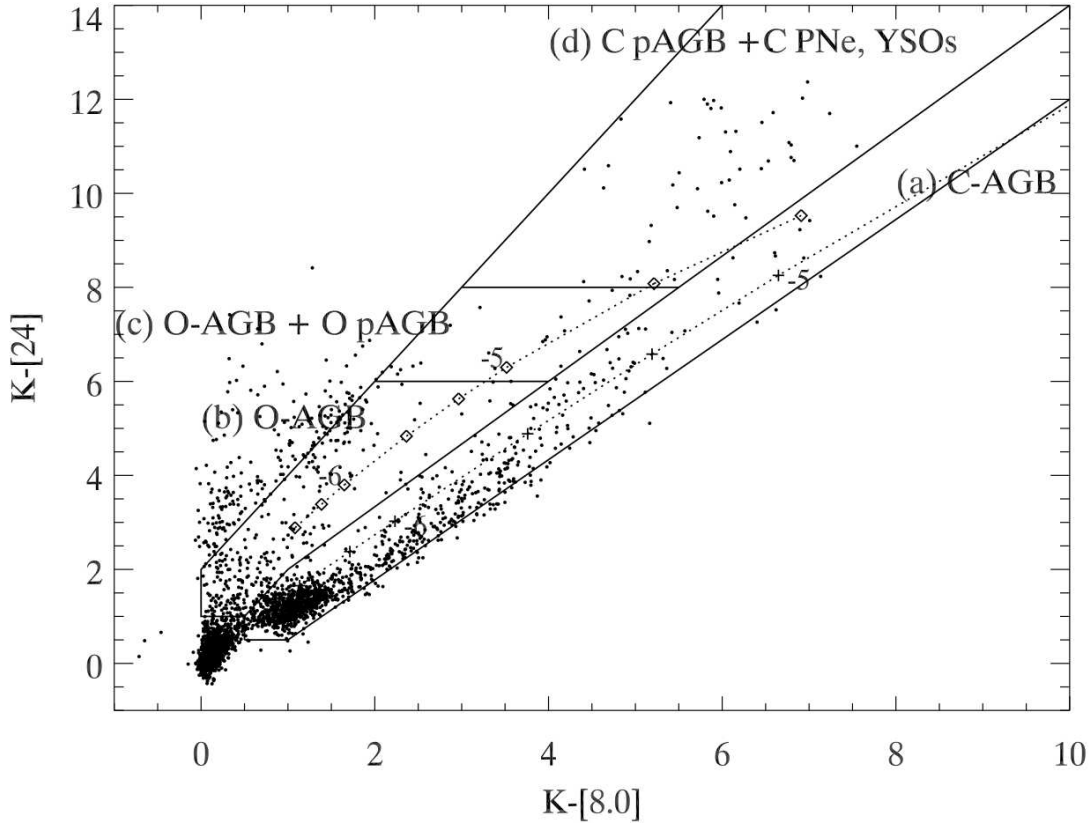


Figure 5. Same as Fig. 3, but for the point sources in the SMC. There are very few oxygen-rich stars with colour redder than $K - [8.0] > 1.8$, which corresponds to a mass-loss rate higher than $> 10^{-6} M_{\odot} \text{ yr}^{-1}$.

SN rates and the progenitor mass, as well as dust mass formed in the SNe themselves.

The SN rates have been estimated for both the LMC and the SMC, using the number and age of the supernova remnants (SNRs) in these galaxies as a starting point. In our previous LMC study (Matsuura et al. 2009), we used SN rates from Mathewson et al. (1983) and Filipovic et al. (1998). The Mathewson et al. (1983) estimate is a factor of two lower than Filipovic et al. (1998). Filipovic et al. (1998)'s study is more recent, so we adopt this value here. Their rate includes both type Ia and II SNe. Tsujimoto et al. (1995) estimated the ratio of type Ia over type II is 0.2–0.3 for both the LMC and the SMC. Combining the SN rate from Filipovic et al. (1998) and type Ia and type II ratio from Tsujimoto et al. (1995), we obtain type SN II rate of one in every 125–143 years in the LMC and one in every 438–500 years in the SMC.

In our previous study of the LMC (Matsuura et al. 2009), we have used the average SN progenitor mass of $8 M_{\odot}$ from SN progenitor surveys in the galaxies (Smartt et al. 2009). Eight solar masses correspond to the lowest range of mass that ends their stellar evolution as SNe. One possibility is that this average progenitor mass might have some bias towards the lowest end of SN progenitors, because they are more numerous than higher mass stars and more frequently detected. We take this possibility into consideration.

A mean mass of high-mass stars is much higher than $8 M_{\odot}$; if we take a mean mass of the initial mass function (Kroupa 2001) with the high mass cut off of $50 M_{\odot}$, the av-

erage mass of high-mass stars would be about $16 M_{\odot}$. We take this to give a maximum possible mass of gas ejection rate per SN.

Considering the progenitor mass range and SN rate, the integrated gas inputs from type II SNe are approximately, $6\text{--}13 \times 10^{-2} M_{\odot} \text{ yr}^{-1}$ for the LMC, and $2\text{--}4 \times 10^{-2} M_{\odot} \text{ yr}^{-1}$ for the SMC.

SNe form dust in their ejecta, however, measured dust masses from SNe and SNRs have a wide range. Mid-infrared observations found the lower limit of dust mass to be about $\sim 10^{-5} M_{\odot}$ (Meikle et al. 2007), but up to $\sim 10^{-2} M_{\odot}$ (Sugerman et al. 2006; Fox et al. 2011). Recently, the Herschel Magellanic Survey (HERITAGE; Meixner et al. 2010) found a large amount of dust in SN 1987A (Matsuura et al. 2011), and its mass is about $0.3\text{--}0.7 M_{\odot}$, showing SNe can form significant dust mass, following a measurements in Galactic SNR, Cas A ($0.08 M_{\odot}$ of dust; Barlow et al. 2010; Sibthorpe et al. 2010). It seems that the measured dust mass does not correlate with the progenitor mass (Otsuka et al. 2011; Gall et al. 2011). In our estimate of the SN dust injection rate, we take two cases, $\sim 10^{-2} M_{\odot}$ as a conservative case, as taken in our previous study (Matsuura et al. 2009). The other case is $0.5 M_{\odot}$ per SNe. This assumes that the dust detected in SN 1987A after 25 years from the explosion would not be destroyed in the later stage by the ISM and SN wind collisions. The dust mass per event brings the dust ejection rate to $7\text{--}400 \times 10^{-5} M_{\odot} \text{ yr}^{-1}$ for the LMC, and $2\text{--}110 \times 10^{-5} M_{\odot} \text{ yr}^{-1}$ for the SMC.

4.3 Other dust and gas sources

There are other possible sources which could contribute to the gas and dust budgets, such as Wolf-Rayet (WR) stars, luminous blue variables (LBVs), novae and OB stars. We briefly discuss their contributions to the budget.

Studies of Galactic WR stars show that late-type (WR9 and WC 10) stars form carbonaceous dust (Williams et al. 1987). In the Magellanic Clouds, such late-type WR stars have not been found yet. Among known WR stars, the LMC WR star (HD 36402; WC 4) was detected at mid-infrared wavelength (Williams 2011), and its mass is estimated to be $1.5 \times 10^{-7} M_{\odot}$. It is not clear what the time scale of this dust formation and ejection rate is, but WR dust input is much smaller than that of AGB stars and SNe combined in the LMC. There is no report of dust formation in SMC WR, so far.

There are just over ten WR stars known in the SMC (Pasemann et al. 2011). Their mass loss is line driven, and the mass-loss rate decreases with metallicity (Kudritzki 2002; Crowther & Hadfield 2006). Assuming each WR star ejects approximately $1 \times 10^{-5} M_{\odot} \text{ yr}^{-1}$ of gas (Crowther 2000), WR stars eject is about $1 \times 10^{-4} M_{\odot} \text{ yr}^{-1}$ of gas into the ISM in the SMC. The LMC WR catalog lists 134 stars (Breysacher et al. 1999) and about $1 \times 10^{-3} M_{\odot} \text{ yr}^{-1}$ of gas is ejected from WR stars into the ISM in the LMC.

There are over 300 OB stars in the SMC (Lamb et al. 2011). If their mass-loss rate is typically about 10^{-8} – $10^{-6} M_{\odot} \text{ yr}^{-1}$ per star (Prinja 1987), the total mass-loss rate is about $\sim 3 \times 10^{-5}$ – $\sim 3 \times 10^{-3} M_{\odot} \text{ yr}^{-1}$. In the LMC, the total mass-loss rate from approximately 1000 OB stars (Bastian et al. 2009) is about $\sim 1 \times 10^{-4}$ – $\sim 1 \times 10^{-2} M_{\odot} \text{ yr}^{-1}$.

Luminous blue variables (LBVs) could potentially make significant amounts of silicate dust (Morris et al. 1999; Gomez et al. 2010). Among the S Dor star catalog of Van Genderen (2001), three LBVs have an infrared excess in the LMC, which are R71, R127 and BAT 99-83 (Bonanos et al. 2009), indicating dust formation in these stars. In the SMC Bonanos et al. (2010) found three LBVs that indicate an infrared excess. However, we found that solely IR data can not distinguish between RSGs and LBVs (Fig.2), so that LBVs are combined together with RSGs in the overall gas and dust budget.

Classical novae can form dust and observations of Galactic novae reported dust mass ranges between 10^{-10} – $10^{-5} M_{\odot}$ depending on the objects (Gehrz et al. 1998). As far as we are aware, there is no report of dust formation in novae in the Magellanic Clouds, so that we do not include novae in the dust budget, at this moment.

Kastner et al. (2006) found two LMC Be stars to have dust in discs. These are probably formed during occasional outbursts. The estimated mass-loss rate was $5 \times 10^{-4} M_{\odot} \text{ yr}^{-1}$ giving the minimum mass injection rate from Be stars into the ISM of $10^{-3} M_{\odot} \text{ yr}^{-1}$. Bonanos et al. (2010) have cross correlated optical spectral surveys of massive stars in the SMC (Evans et al. 2004), and found that five B[e] stars have infrared excess. They could have contributed approximately $1 \times 10^{-5} M_{\odot} \text{ yr}^{-1}$ of dust.

Two RCrB stars have an infrared excess. One is MSX LMC 439 (Tisserand et al. 2009) and the other is MSX LMC 1795 (Soszyński et al. 2009). Clayton et al. (2011) studied another LMC RCrB star, HV 2671. In our estimate, we in-

tegrate RCrB stars into carbon-rich AGB stars, as they can not be distinguished from IR data only (Fig.2).

AGB stars have one more chemical type, on top of oxygen-rich (M-type) and carbon-rich (C-type): S-type stars. They have a carbon-to-oxygen ratio almost equal to unity. Their dust composition is diverse: FeO, FeS, silicate (Zijlstra et al. 2004; Smolders et al. 2012). The number of S-type stars is small ($\sim 1\%$ in the Galaxy) among AGB stars, so their contributions to the total gas and dust budget is negligible.

5 DISCUSSIONS

5.1 Global gas and dust budget of the SMC

In the SMC, the total gas injection rate from AGB stars, RSGs and SNe is 0.02 – $0.04 M_{\odot} \text{ yr}^{-1}$. This largely relies on the gas ejected from SNe.

We compare this gas injected from SNe and evolved stars into the ISM with gas consumed by star formation. Kennicutt & Hodge (1986) estimated the current SMC starformation rate of $0.08 M_{\odot} \text{ yr}^{-1}$. In the SMC ISM, gas consumed by the starformation exceeds the gas injected from evolved stars and SNe (0.02 – $0.04 M_{\odot} \text{ yr}^{-1}$) into the ISM. This is similar to what has been found in the LMC, though the deficit in the LMC is much larger (about 0.1 – $0.2 M_{\odot} \text{ yr}^{-1}$).

The majority of the ISM gas in the SMC is present in the form of HI and its mass is $4 \times 10^8 M_{\odot}$ (Stanimirović et al. 1999; Bolatto et al. 2011). A large ISM reservoir could sustain the star formation, despite a deficit in the gas injection rate, at least on a few Gyr time scale. Unless there is a gas infall from an external source, the starformation rate will decline.

Similarly, SNe and AGB stars are important dust sources in the SMC. SNe could contribute to a dust injection of 2 – $110 \times 10^{-5} M_{\odot} \text{ yr}^{-1}$ into the ISM, while AGB stars and RSGs contribute about $1 \times 10^{-5} M_{\odot} \text{ yr}^{-1}$ of dust mass.

In the Milky Way, the lifetime of dust is estimated to be 6×10^8 years and 4×10^8 years for carbonaceous and silicate dust grains, respectively (Jones et al. 1996). The lifetime of dust grains is constrained by their destruction by fast SN shocks and the dust lifetime correlates with the SN Ia+II rate per surface area (Dwek 1998). The Galactic SN rate is estimated to be one in every 50 years (Diehl et al. 2006). This rate includes type Ib/c and II, but in practice type II dominates. The type Ia rate in the Milky Way is about 0.3 per century (Matteucci et al. 2009), so that the total SN Ia and II rate is about one event in every 45 years in the Milky Way. The SMC has a rate of one event every 350 years, and in the LMC the rate is one event every 100 years (Filipovic et al. 1998). To calculate the SN rate per surface area, we use the half-light radius ($r_{1/2}$) of a galaxy as a measure of the surface area, which we take from Tolstoy et al. (2009). The estimated dust lifetime would be 5×10^8 years and 3×10^8 years for carbonaceous and silicate dust grains, respectively in the LMC, and 17×10^8 years and 11×10^8 years in the SMC. In the SMC, the overall lifetime of the dust would be about 1.4 Gyrs. This assumes an almost constant SN rate and starformation rate over such a long period, which will be discussed in Sect. 5.2. In the SMC, about 4×10^4 – $1 \times 10^6 M_{\odot}$

of dust has been accumulated over the 1.4 Gyr history of the SMC.

The estimated dust mass in the SMC ISM is $3 \times 10^5 M_{\odot}$ (Leroy et al. 2007). If the dust lifetime in the SMC ISM is as long as 1.4 Gyrs on average, dust present in the SMC ISM may mainly originate from stellar dust.

The obvious uncertainty in this estimate is the lifetime of dust. The half-light radius is an indicator of the galaxy size, but the LMC and the SMC are irregular galaxies, and the actual SN rate per volume would not be so simple to estimate. Furthermore, SNe might affect dust destruction in the SN vicinity only, and dust in the remaining regions might survive. The uneven distribution of dust could bring diverse life-time of dust. It seems that the dust lifetime largely depends on the local condition of the galaxies, and more sophisticated calculations are needed.

It has been proposed that dust condensation in molecular clouds could be a dominant source of ISM dust in the Milky Way or high-redshift galaxies (Tielens 2006; Draine 2009; Mattsson 2011). These galaxies probably contain many molecular clouds within. The SMC is known to have a low molecular content (Israel 1997), so that dust condensation in the molecular clouds may not be as high as in the Milky Way.

The key to understand the evolution of ISM dust is to understand the formation and destruction processes imposed by SNe. It is now pausable to determine dust formation and destruction in SNe, using the current missions/projects, such as Herschel, SOFIA and ALMA, but also future space missions (JWST and SPICA; Tanaka et al. 2012). Also we need to find constraints for grain growth in molecular clouds based on observations.

5.2 Comparison between the LMC and the SMC

In the SMC SNe are a more important gas source to the ISM than AGB stars and RSGs. The difference between them is a factor of 14–29. In the LMC SNe have higher gas feedback rates than AGB stars and RSGs but the difference is only by a factor of 4–9. AGB mass-loss rates have uncertainties of a factor of three at least (Groenewegen et al. 2007), and the gas-to-dust mass ratio could have a factor of three uncertainties (van Loon 2000). The LMC difference is negligible, but the one in the SMC is not. There is a difference in the main gas sources in the LMC and SMC. The SMC has more gas feedback from high-mass stars than the LMC.

The initial mass function (Kroupa 2001) shows that equivalent mass should be distributed to high-mass stars ($>8 M_{\odot}$) and low- and intermediate-mass stars ($1-8 M_{\odot}$). At the event of stellar death, high-mass stars could return most of their mass into the ISM. Many low- and intermediate-mass stars end their lives as white dwarfs, and their masses are about $0.6 M_{\odot}$ (Weidemann 1990), thus 40–92 % of mass is returned to the ISM. During a constant starformation rate period, the ratio of ISM gas feedback from high-mass stars against low- and intermediate-mass stars should be about 3:2. The measured ratio shows that SMC has an excess of gas feedback from high-mass stars beyond the IMF.

The LMC and SMC have experienced more or less similar starformation histories (Harris & Zaritsky 2004, 2009), but the SMC has an enhanced starformation history by a fac-

tor of four in recent times in the last 12 Myrs. That could result in a more efficient gas injection rate from SNe.

Additionally, the lower metallicity can cause lower dust driven winds, at least for oxygen-rich AGB stars and red supergiants (Bowen & Willson 1991; Marshall et al. 2004). The metallicities of the LMC and the SMC are about half and the quarter of Solar (Monk et al. 1988). That could be another reason that there is a more efficient SN gas feedback in the SMC, because of the relatively smaller contribution of oxygen-rich AGB stars and red supergiants.

5.3 PAHs in the SMC

Carbon-rich AGB stars are considered to be the source of PAHs found the ISM (Allamandola et al. 1989; Cherchneff et al. 1992). PAHs are formed using C_2H_2 as a parent molecule in chemical reactions. In the circumstellar envelope of carbon-rich AGB stars, carbon atoms are tied up in CO first, and use up all oxygen, and the excess carbon formed carbonaceous dust and carbon-bearing molecules.

From our measured carbon-rich AGB gas injection rate, we can estimate the upper limit of PAH mass injected from carbon stars. The gas injection rate from carbon-rich AGB stars is $0.7 \times 10^{-2} M_{\odot} \text{ yr}^{-1}$. The C_2H_2 fractional abundance is approximately 10^{-5} in the Milky Way (Howe & Millar 1996). This can be has a factor of few higher, depending on how the metallicities of the galaxies affect the amount of excess carbon in the stars (Matsuura et al. 2005), and to be predicted to be about 10^{-4} (Woods et al. 2012) in the Magellanic Clouds. The maximum PAH injection rate, if all C_2H_2 is eventually converted into PAHs, is $0.7 \times 10^{-6} M_{\odot} \text{ yr}^{-1}$.

The average fractional abundance of PAHs in the SMC is 0.6 % with respect to the total dust mass (Sandstrom et al. 2010). The estimated PAH mass in the SMC to be about $1800 M_{\odot}$.

The lifetime of PAHs is shorter than amorphous carbon. In the Milky Way, the estimated lifetime of PAHs is $1.4-1.6 \times 10^8$ years (Micelotta et al. 2010). In the SMC, the SN rate is lower, and the lifetime of PAHs can be as long as a few 10^8 years. The PAH injection rate from carbon-rich AGB stars is so low that the expected PAH mass from AGB stars would be much lower than $100 M_{\odot}$. PAHs in the SMC require efficient in the ISM or in-falling into the SMC. PAH formation needs ISM processing.

6 CONCLUSIONS

We have measured the total gas and dust injection rates from AGB stars, red supergiants, and also estimated these rates from supernovae. The total gas injection from stellar deaths is about $2-4 \times 10^{-2} M_{\odot} \text{ yr}^{-1}$ into the ISM. This is slightly smaller than the current gas consumption in the ISM by starformation, which is $\sim 8 \times 10^{-2} M_{\odot} \text{ yr}^{-1}$. The galaxy has a large gas reservoir the moment, so that it can sustain high starformation rate at present. Eventually the starformation rate is going to decline, unless an external source provides gas infall into the SMC.

AGB stars and red supergiants are important sources of dust in the SMC. Dust production in SNe is largely uncertain, so is the lifetime of dust. Within the current uncertain-

ties in quantities, dust present in the ISM can be explained as being stellar in origin.

PAHs in the ISM can not be explained to have originated only from carbon-rich AGB stars. The lifetime of PAHs is too short, compared with the supply from carbon-rich AGB stars. PAHs require formation process in the ISM.

REFERENCES

- Allamandola L. J., Tielens A. G. G. M., Barker J. R., 1989, *ApJS*, 71, 733
- Barlow M. J., Krause O., Swinbank B. M., et al. 2010, *A&A*, 518, L138
- Bastian N., Gieles M., Ercolano B., Gutermuth R., 2009, *MNRAS*, 392, 868
- Blanco V. M., Blanco B. M., McCarthy M. F., 1980, *ApJ*, 242, 938
- Blum R. D., Mould J. R., Olsen K. A., et al. 2006, *AJ*, 132, 2034
- Bolatto A. D., Leroy A. K., Jameson K., et al. 2011, *ApJ*, 741, 12
- Bolatto A. D., Simon J. D., Stanimirović S., et al. 2007, *ApJ*, 655, 212
- Bonanos A. Z., Lennon D. J., Köhlinger F., et al. 2010, *AJ*, 140, 416
- Bonanos A. Z., Massa D. L., Sewilo M., et al. 2009, *AJ*, 138, 1003
- Bowen G. H., Willson L. A., 1991, *ApJ*, 375, L53
- Boyer M. L., Srinivasan S., Riebel D., et al. 2012, *ApJ*, 748, 40
- Breysacher J., Azzopardi M., Testor G., 1999, *A&AS*, 137, 117
- Bruzual G., Charlot S., 2003, *MNRAS*, 344, 1000
- Calura F., Pipino A., Matteucci F., 2008, *A&A*, 479, 669
- Cherchneff I., Barker J. R., Tielens A. G. G. M., 1992, *ApJ*, 401, 269
- Cioni M.-R. L., Marquette J.-B., Loup C., Azzopardi M., Habing H. J., Lasserre T., Lesquoy E., 2001, *A&A*, 377, 945
- Clayton G. C., de Marco O., Whitney B. A., et al. 2011, *AJ*, 142, 54
- Crowther P. A., 2000, *A&A*, 356, 191
- Crowther P. A., Hadfield L. J., 2006, *A&A*, 449, 711
- Diehl R., Halloin H., Kretschmer K., et al. 2006, *Nature*, 439, 45
- Draine B. T., 2009, *ASP Conference Series*, 414, 453
- Dunne L., Gomez H. L., da Cunha E., et al. 2011, *MNRAS*, 417, 1510
- Dwek E., 1998, *ApJ*, 501, 643
- Evans C. J., Howarth I. D., Irwin M. J., Burnley A. W., Harries T. J., 2004, *MNRAS*, 353, 601
- Ferrarotti A. S., Gail H.-P., 2006, *A&A*, 447, 553
- Filipovic M. D., Pietsch W., Haynes R. F., et al. 1998, *A&AS*, 127, 119
- Fox O. D., Chevalier R. A., Skrutskie M. F., et al. 2011, *ApJ*, 741, 7
- Gall C., Hjorth J., Andersen A. C., 2011, *A&AR*, 19
- Galliano F., Madden S. C., Jones A. P., Wilson C. D., Bernard J.-P., 2005, *A&A*, 434, 867
- Gehrz R. D., 1989, *IAUS*, 135, 445
- Gehrz R. D., Truran J. W., Williams R. E., Starrfield S., 1998, *PASP*, 110, 3
- Gielen C., Van Winckel H., Reyniers M., et al. 2009, *A&A*, 508, 1391
- Gomez H. L., Clark C. J. R., Nozawa T., et al. 2012, *MNRAS*, 420, 3557
- Gomez H. L., Krause O., Barlow M. J., et al. 2012, *The Astrophysical Journal*, 760, 96
- Gomez H. L., Vlahakis C., Stretch C. M., et al. 2010, *MNRAS*, 401, L48
- Gordon K. D., Meixner M., Meade M. R., et al. 2011, *AJ*, 142, 102
- Groenewegen M. A. T., Sloan G. C., Soszynski I., Petersen E. A., 2009, *A&A*, 506, 1277
- Groenewegen M. A. T., Wood P. R., Sloan G. C., et al. 2007, *MNRAS*, 376, 313
- Habing H. J., 1996, *A&AR*, 7, 97
- Harris J., Zaritsky D., 2004, *AJ*, 127, 1531
- Harris J., Zaritsky D., 2009, *AJ*, 138, 1243
- Henize K. G., 1955, *APJS*, 2, 315
- Howe D. A., Millar T. J., 1996, *MNRAS*, 282, L21
- Hughes S. M. G., 1989, *AJ*, 97, 1634
- Israel F. P., 1997, *A&A*, 328, 471
- Ita Y., Onaka T., Kato D., et al. 2008, *PASJ*, 60, 435
- Jones A. P., Tielens A. G. G. M., Hollenbach D. J., 1996, *ApJ*, 469, 740
- Jura M., Kleinmann S. G., 1989, *ApJ*, 341, 359
- Kastner J. H., Buchanan C. L., Sargent B., Forrest W. J., 2006, *ApJ*, 638, L29
- Kemper F., Woods P. M., Antoniou V., et al. 2010, *PASP*, 122, 683
- Kennicutt R. C., Hodge P. W., 1986, *ApJ*, 306, 130
- Kjær K., Leibundgut B., Fransson C., Jerkstrand A., Spyromilio J., 2010, *A&A*, 517, A51
- Kodama T., Arimoto N., 1997, *A&A*, 320, 41
- Kontizas E., Dapergolas A., Morgan D. H., Kontizas M., 2001, *A&A*, 369, 932
- Kozłowski S., Kochanek C. S., 2009, *ApJ*, 701, 508
- Kroupa P., 2001, *MNRAS*, 322, 231
- Kudritzki R. P., 2002, *ApJ*, 577, 389
- Lamb J. B., Oey M. S., Graus A. S., Segura-Cox D. M., 2011, *ASP Conf*, 440, 73
- Le Bertre T., Matsuura M., Winters J. M., Murakami H., Yamamura I., Freund M., Tanaka M., 2001, *A&A*, 376, 997
- Le Bertre T., Winters J. M., 1998, *A&A*, 334, 173
- Leroy A., Bolatto A., Stanimirović S., Mizuno N., Israel F., Bot C., 2007, *ApJ*, 658, 1027
- McCumber M. P., Garnett D. R., Dufour R. J., 2005, *APJS*, 130, 1083
- Marshall J. R., van Loon J. T., Matsuura M., Wood P. R., Zijlstra A. A., Whitelock P. A., 2004, *MNRAS*, 355, 1348
- Mathewson D. S., Ford V. L., Dopita M. A., Tuohy I. R., Long K. S., Helfand D. J., 1983, *ApJS*, 51, 345
- Matsuura M., Barlow M. J., Zijlstra A. A., et al. 2009, *MNRAS*, 396, 918
- Matsuura M., Dwek E., Meixner M., et al. 2011, *Science*, 333, 1258
- Matsuura M., Sloan G. C., Bernard-Salas J., Volk K., Hrivnak B. J., 2011, *APN*, 5, 97
- Matsuura M., Zijlstra A. A., van Loon J. T., et al. 2005, *A&A*, 434, 691

- Matteucci F., Spitoni E., Recchi S., Valiante R., 2009, *A&A*, 501, 531
- Mattsson L., 2011, *MNRAS*, 414, 781
- Meikle W. P. S., Mattila S., Pastorello A., et al. 2007, *ApJ*, 665, 608
- Meixner M., Galliano F., Hony S., et al. 2010, *A&A*, 518, L71
- Meixner M., Gordon K. D., Indebetouw R., et al. 2006, *AJ*, 132, 2268
- Micelotta E. R., Jones A. P., Tielens A. G. G. M., 2010, *A&A*, 510, A36
- Monk D. J., Barlow M. J., Clegg R. E. S., 1988, *MNRAS*, 234, 583
- Morgan H. L., Edmunds M. G., 2003, *MNRAS*, 343, 427
- Morris P. W., Waters L. B. F. M., Barlow M. J., et al. 1999, *Nature*, 402, 502
- Nikolaev S., Weinberg M. D., 2000, *ApJ*, 542, 804
- Nozawa T., Kozasa T., Umeda H., Maeda K., Nomoto K., 2003, *ApJ*, 598, 785
- Otsuka M., Meixner M., Panagia N., et al. 2011, *ApJ*, 744, 26
- Pagel B. E. J., Tautvaisiene G., 1998, *MNRAS*, 299, 535
- Pasemann D., Röhling U., Hamann W.-R., 2011, *Bulletin de la Societe Royale des Sciences de Liege*, 80, 180
- Prinja R. K., 1987, *MNRAS*, 228, 173
- Reid N., Glass I. S., Catchpole R. M., 1988, *MNRAS*, 232, 53
- Sandstrom K. M., Bolatto A. D., Draine B. T., Bot C., Stanimirović S., 2010, *ApJ*, 715, 701
- Sanduleak N., Philip A. G. D., 1977, *PASP*, 89, 792
- Sibthorpe B., Ade P. A. R., Bock J. J., et al. 2010, *ApJ*, 719, 1553
- Skrutskie M. F., Cutri R. M., Stiening R., et al. 2006, *AJ*, 131, 1163
- Sloan G. C., Matsuura M., Zijlstra A. A., et al. 2009, *Science*, 323, 353
- Smartt S. J., Eldridge J. J., Crockett R. M., Maund J. R., 2009, *MNRAS*, 395, 1409
- Smolders K., Neyskens P., Blommaert J. A. D. L., et al. 2012, *A&A*
- Soszyński I., Udalski A., Szymanski M. K., Kubiak M., Pietrzynski G., Wyrzykowski Ł., Szewczyk O., Ulaczyk K., Poleski R., 2009, *Acta Astronomica*, 59, 335
- Srinivasan S., Meixner M., Leitherer C., et al. 2009, *AJ*, 137, 4810
- Stanimirović S., Staveley-Smith L., Dickey J. M., Sault R. J., Snowden S. L., 1999, *MNRAS*, 302, 417
- Sugerman B. E. K., Ercolano B., Barlow M. J., et al. 2006, *Science*, 313, 196
- Tanaka M., Nozawa T., Sakon I., Onaka T., Arimatsu K., Ohsawa R., Maeda K., Wada T., Matsuhara H., Kaneda H., 2012, *ApJ*, 749, 173
- Tielens A. G. G. M., 2006, *Sterne und Weltraum*, 45, 106
- Tielens A. G. G. M., Waters L. B. F. M., Bernatowicz T. J., 2005, *Chondrites and the Protoplanetary Disk*, 341, 605
- Tisserand P., Wood P. R., Marquette J.-B., et al. 2009, *A&A*, 501, 985
- Tolstoy E., Hill V., Tosi M., 2009, *ARA&A*, 47, 371
- Tsujimoto T., Nomoto K., Yoshii Y., Hashimoto M., 1995, *MNRAS*, 277, 945
- Valiante R., Schneider R., Bianchi S., Andersen A. C., 2009, *MNRAS*, 397, 1661
- Van Genderen A. M., 2001, *A&A*, 366, 508
- van Loon J. T., 2000, *A&A*, 354, 125
- Volk K., Hrivnak B. J., Matsuura M., et al. 2011, *ApJ*, 735, 127
- Weidemann V., 1990, *ARA&A*, 28, 103
- Werner M. W., Roellig T. L., Low F. J., et al. 2004, *APJS*, 154, 1
- Westerlund B. E., 1990, *A&AR*, 2, 29
- Westerlund B. E., Olander N., Hedin B., 1981, *A&AS*, 43, 267
- Whitelock P. A., Menzies J., Feast M. W., Marang F., Carter B., Roberts G., Catchpole R., Chapman J., 1994, *MNRAS*, 267, 711
- Williams P. M., 2011, *Bulletin de la Societe Royale des Sciences de Liege*, 80, 195
- Williams P. M., van der Hucht K. A., The P. S., 1987, *A&A*, 182, 91
- Wood P. R., Bessell M. S., Fox M. W., 1983, *ApJ*, 272, 99
- Wood P. R., Bessell M. S., Paltoglou G., 1985, *ApJ*, 290, 477
- Wood P. R., Whiteoak J. B., Hughes S. M. G., Bessell M. S., Gardner F. F., Hyland A. R., 1992, *ApJ*, 397, 552
- Woods P. M., Oliveira J. M., Kemper F., et al. 2011, *MNRAS*, 411, 1597
- Woods P. M., Walsh C., Cordiner M. A., Kemper F., 2012, *MNRAS*, 426, 2689
- Zhukovska S. V., Gail H.-P., Tieloff M., 2008, *A&A*, 479, 453
- Zijlstra A. A., Bedding T. R., Markwick A. J., et al. 2004, *MNRAS*, 352, 325